Electronic Supplementary Material (ESI) for Chemical Science.

Electronic Supplementary Information (ESI) for

$Cs_3VO(O_2)_2CO_3$: An exceptionally thermostable carbonatoperoxovanadate with the extremely large second-harmonic generation response

Guohong Zou,*[a] Zhien Lin,[a] Hongmei Zeng,[a] Hongil Jo,[b] Seong-Ji Lim,[c] Tae-Soo You[c] and Kang Min Ok*[b]

[a]College of Chemistry, Sichuan University, Chengdu, 610064, P. R. China.

[b]Department of Chemistry, Chung-Ang University, Seoul 06974, Republic of Korea

[c]Department of Chemistry, Chungbuk National University, Cheongju, Chungbuk, 28644, Republic of Korea

*E-mail: zough@scu.edu.cn; kmok@cau.ac.kr

Table of contents

Section S1. Materials and Methods

Synthesis. Cs_2CO_3 (99.5%), V_2O_5 (99.0%), and H_2O_2 (40%) were purchased from Sinopharm and used as received. Single crystals of $Cs_3VO(O_2)_2CO_3$ were grown through a solution-evaporation method. $CsVO_3$ was initially synthesized by a high temperature solid state reaction with a mixture of Cs_2CO_3 and V_2O_5 at a molar ratio of Cs_2CO_3/V_2O_5 = 1:1 at 420 °C for 40 h. After that, $CsVO_3$ (2.0 g), Cs_2CO_3 (10.0 g), and 3.0 mL of H_2O_2 (40%) were dissolved in 50 mL of distilled water. The resulting faint yellow transparent solution was then transferred to a refrigerator and slowly evaporated at 5 °C. Yellow plate-like crystals were grown in about 20 days (see Fig. S1)

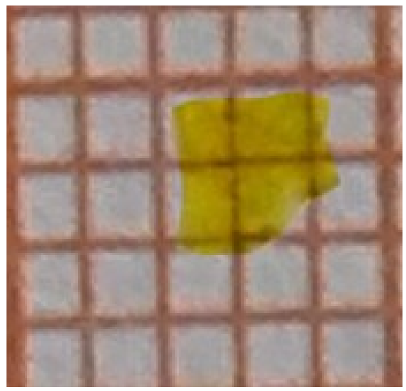

Fig. S1. Photograph of $Cs_3VO(O_2)_2CO_3$ crystal

Instrumentations. Single crystal X-ray diffraction data of $Cs_3VO(O_2)_2CO_3$ were collected at room temperature on a Bruker SMARTBREEZE diffractometer equipped with a 1K CCD area detector using graphite monochromated Mo Kα radiation. The structure was solved by a direct method and refined by full-matrix least-squares fitting on F^2 using SHELX-97.[S1] All of the structures were verified using the ADDSYM algorithm from the program PLATON,[S2] and no higher symmetries were found. Relevant crystallographic data and details of the experimental conditions for $Cs_3VO(O_2)_2CO_3$ are summarized in Table S1. Atomic coordinates and isotropic displacement parameters are listed in Table S2. Selected bond lengths and angles for $Cs_3VO(O_2)_2CO_3$ are listed in Table S3. The powder X-ray diffraction (PXRD) data were collected on a Bruker D8-Advance diffractometer using Cu K_α radiation at room temperature with 40 kV and 40 mA in the angular range of 2θ = 5–70° with a scan step width of 0.05° and a fixed time of 0.2 s. The powder XRD patterns for the pure samples of $Cs_3VO(O_2)_2CO_3$ showed good agreement with the calculated XRD patterns from the single-crystal model (see Figure S2). Thermogravimetric analysis (TGA) was conducted on a Netzsch STA 409 PC. The crystal sample (10–15 mg) were enclosed in a platinum crucible and heated from room temperature to 1000 °C at a rate of 10 °C/min under a constant flow of air gas. Infrared spectrum of the sample was recorded on a Thermo Scientific Nicolet 6700 FT-IR spectrometer in the 400–4000 cm^{-1} range, with the sample embedded in a KBr matrix. UV-vis diffuse reflectance spectrum was obtained on a Varian Cary 500 scan UV-vis-NIR spectrophotometer over the spectral range 200–2500 nm at room temperature. The transmittance spectrum was measured from 200 to 800 nm using an unpolished $Cs_3VO(O_2)_2CO_3$ crystal. The reflectance spectrum was transformed into the absorbance spectrum using the Kubelka–Munk function.[S3,S4] Scanning electron microscope (SEM)/energy-dispersive analysis by X-ray (EDX) analyses have been performed using a Hitachi S-3400N/Horiba Energy EX-250 instruments. EDX for

$Cs_3VO(O_2)_2CO_3$ reveals Cs:V ratio of approximately 3.2:1.1 (see Fig. S6). Powder SHG measurements were carried out using the experimental method adapted from that reported by Kurtz and Perry[S5] with 1064 nm radiation. Since SHG efficiencies were known to be strongly dependent on particle size, polycrystalline samples were ground and sieved into the following particle size ranges: 20–45, 45–63, 63–75, 75–90, 90–125, 125–150, 150–200, 200–250 μm. In order to make relevant comparisons with known SHG materials, crystalline KDP and $KSrCO_3F$ were also ground and sieved into the same particle size ranges. All of the sieved samples with different particle sizes were packed into distinct capillary tubes. The reflected green SHG light with 532 nm was collected and detected using a photomultiplier tube (Hamamatsu). To detect only the SHG light, a 532 nm narrow band-pass interference filter was attached to the front of the tube. The generated SHG signal was monitored using a digital oscilloscope (Tektronix TDS1032). This procedure was then repeated using the standard nonlinear optical materials, i.e., KDP and the ratio of the second-harmonic intensity outputs was calculated. No index-matching fluid was used in any of the experiments. A detailed description of the methodology and the equipment used has been previously published.[S5]

Table S1. Crystallographic Data for $Cs_3VO(O_2)_2CO_3$

formula	$Cs_3VO(O_2)_2CO_3$
fw	589.68
space group	*Cm* (No. 8)
a (Å)	9.447(3)
b (Å)	10.129(3)
c (Å)	6.1571(18)
β (°)	123.42(3)
V (Å^3)	491.7(3)
Z	2
T (K)	298.0(2)
λ (Å)	0.71073
ρ_{calcd} (g cm^{-3})	3.983
$R(F)^a$	0.026
$R_w(F_o^2)^b$	0.097
Flack param.	0.08(7)

$^aR(F) = \Sigma ||F_o| - |F_c|| / \Sigma |F_o|$. $^bR_w(F_o^2) = [\Sigma w(F_o^2 - F_c^2)^2 / \Sigma w(F_o^2)^2]^{1/2}$.

Table S2. Atomic Coordinates and Equivalent Isotropic Displacement Parameters (Å^2) for $Cs_3VO(O_2)_2CO_3$.

	x	*y*	*z*	$U_{eq}{}^a$	BVS
Cs1	0.68523 (10)	0.21964 (7)	0.15364 (14)	0.0264 (3)	1.32
Cs2	1.14643 (9)	0.0000	0.59743 (12)	0.0267 (3)	1.12
V1	0.5560 (3)	0.0000	0.5225 (4)	0.0186 (6)	5.34
O1	0.4516 (15)	0.0000	0.207 (2)	0.027 (3)	2.01
O2	0.9481 (9)	0.3756 (9)	0.6053 (16)	0.0253 (18)	1.45
O3	0.7936 (15)	0.0000	0.590 (2)	0.029 (3)	1.98
O4	1.0407 (15)	0.0000	0.980 (3)	0.025 (2)	2.04
O5	0.7903 (13)	0.0000	0.946 (2)	0.025 (3)	2.09
O6	1.0779 (10)	0.3065 (10)	0.5768 (18)	0.0273 (18)	1.08
C1	0.8812 (19)	0.0000	0.852 (3)	0.023 (3)	3.92

$^aU_{eq}$ is defined as one third of the trace of the orthogonalized U_{ij} tensor.

Table S3. Selected Bond Distances (Å) and Angles (°) for $Cs_3VO(O_2)_2CO_3$.

Cs1—O2	2.965 (8)	V1—O5	2.311 (11)
Cs1—O5^{i}	2.995 (7)	V1—O1	1.624 (11)
Cs1—O2^{ii}	3.003 (8)	V1—O2^{x}	1.860 (8)
Cs1—O4^{iii}	3.076 (5)	V1—O2^{iv}	1.860 (8)
Cs1—O6^{ii}	3.121 (9)	V1—O6^{iv}	1.980 (10)
Cs1—O3	3.192 (9)	V1—O6^{x}	1.980 (10)
Cs1—O6	3.267 (9)	V1—O3	2.044 (11)
Cs1—O1	3.275 (10)	V1—O1	1.624 (11)
Cs1—O6^{iv}	3.286 (9)	V1—O2^{x}	1.860 (8)
Cs1—O1^{v}	3.687 (8)	V1—O2^{iv}	1.860 (8)
Cs2—O4	3.023 (13)	V1—O6^{iv}	1.980 (10)
Cs2—O2^{vi}	3.092 (8)	O2—Cs1^{xiv}	3.003 (8)
Cs2—O2^{vii}	3.092 (8)	O2—Cs2^{xv}	3.092 (8)
Cs2—O6^{viii}	3.159 (10)	O3—C1	1.345 (18)
Cs2—O6	3.159 (10)	O3—Cs1^{viii}	3.192 (9)

Cs2—O1^{ix}	3.237 (11)	O4—C1	1.258 (18)
Cs2—O3	3.309 (11)	O4—Cs1^{xiv}	3.076 (5)
Cs2—O4^{i}	3.357 (13)	O4—Cs1^{xvi}	3.076 (5)
Cs2—O5^{i}	3.541 (11)	O4—Cs2^{xi}	3.357 (13)
O2—Cs1—O5^{i}	119.5 (3)	O5—C1	1.27 (2)
O2—Cs1—O2^{ii}	161.2 (2)	O5—Cs1^{xi}	2.995 (7)
O5^{i}—Cs1—O2^{ii}	59.9 (3)	O6^{iv}—V1—O3	88.0 (2)
O2—Cs1—O4^{iii}	79.4 (3)	O6^{x}—V1—O3	88.0 (2)
O5^{i}—Cs1—O4^{iii}	136.5 (3)	O1—V1—O5	157.4 (5)
O2^{ii}—Cs1—O4^{iii}	89.6 (3)	O2^{x}—V1—O5	91.1 (3)
O2—Cs1—O6^{ii}	133.8 (2)	O2^{iv}—V1—O5	91.1 (3)
O5^{i}—Cs1—O6^{ii}	55.1 (3)	O6^{iv}—V1—O5	82.1 (3)
O2^{ii}—Cs1—O6^{ii}	28.3 (2)	O6^{x}—V1—O5	82.1 (3)
O4^{iii}—Cs1—O6^{ii}	83.0 (3)	O3—V1—O5	60.6 (4)
O2—Cs1—O3	82.4 (3)	O1—V1—Cs1^{viii}	58.2 (3)
O5^{i}—Cs1—O3	79.3 (2)	O2^{x}—V1—Cs1^{viii}	99.8 (3)
O2^{ii}—Cs1—O3	114.7 (2)	O2^{iv}—V1—Cs1^{viii}	163.4 (3)
O4^{iii}—Cs1—O3	144.2 (3)	O6^{iv}—V1—Cs1^{viii}	129.7 (3)
O6^{ii}—Cs1—O3	130.6 (2)	O6^{x}—V1—Cs1^{viii}	59.2 (3)
O2—Cs1—O6	27.4 (2)	O3—V1—Cs1^{viii}	56.5 (3)
O5^{i}—Cs1—O6	92.4 (3)	O5—V1—Cs1^{viii}	104.4 (2)
O2^{ii}—Cs1—O6	143.1 (2)	O1—V1—Cs1	58.2 (3)
O4^{iii}—Cs1—O6	96.9 (3)	O2^{x}—V1—Cs1	163.4 (3)
O6^{ii}—Cs1—O6	116.4 (3)	O2^{iv}—V1—Cs1	99.8 (3)
O3—Cs1—O6	79.6 (3)	O6^{iv}—V1—Cs1	59.2 (3)
O2—Cs1—O1	122.0 (3)	O6^{x}—V1—Cs1	129.7 (3)
O5^{i}—Cs1—O1	86.5 (2)	O3—V1—Cs1	56.5 (3)
O2^{ii}—Cs1—O1	76.6 (3)	O5—V1—Cs1	104.4 (2)
O4^{iii}—Cs1—O1	117.9 (3)	Cs1^{viii}—V1—Cs1	71.08 (5)
O6^{ii}—Cs1—O1	104.0 (3)	O1—V1—Cs1^{xi}	144.45 (15)

O3—Cs1—O1	50.5 (3)	$O2^{x}$—V1—$Cs1^{xi}$	91.7 (3)
O6—Cs1—O1	129.4 (3)	$O2^{iv}$—V1—$Cs1^{xi}$	44.3 (3)
O2—Cs1—$O6^{iv}$	76.4 (2)	$O6^{iv}$—V1—$Cs1^{xi}$	49.0 (3)
$O5^{i}$—Cs1—$O6^{iv}$	126.8 (2)	$O6^{x}$—V1—$Cs1^{xi}$	115.7 (3)
$O2^{ii}$—Cs1—$O6^{iv}$	120.0 (2)	O3—V1—$Cs1^{xi}$	95.0 (3)
$O4^{iii}$—Cs1—$O6^{iv}$	94.5 (3)	O5—V1—$Cs1^{xi}$	47.18 (18)
$O6^{ii}$—Cs1—$O6^{iv}$	147.8 (3)	$Cs1^{viii}$—V1—$Cs1^{xi}$	149.86 (7)
O3—Cs1—$O6^{iv}$	51.1 (3)	Cs1—V1—$Cs1^{xi}$	102.98 (3)
O6—Cs1—$O6^{iv}$	95.7 (3)	O1—V1—$Cs1^{xii}$	144.45 (15)
O1—Cs1—$O6^{iv}$	49.2 (3)	$O2^{x}$—V1—$Cs1^{xii}$	44.3 (2)
O2—Cs1—$O1^{v}$	47.8 (2)	$O2^{iv}$—V1—$Cs1^{xii}$	91.7 (3)
$O5^{i}$—Cs1—$O1^{v}$	103.9 (2)	$O6^{iv}$—V1—$Cs1^{xii}$	115.7 (3)
$O2^{ii}$—Cs1—$O1^{v}$	113.4 (2)	$O6^{x}$—V1—$Cs1^{xii}$	49.0 (3)
O5—V1—$Cs1^{xii}$	47.18 (18)	O3—V1—$Cs1^{xii}$	95.0 (3)

Symmetry codes: (i) x, y, z−1; (ii) x−1/2, −y+1/2, z−1; (iii) x−1/2, y+1/2, z−1; (iv) x−1/2, −y+1/2, z; (v) x+1/2, y+1/2, z; (vi) x+1/2, −y+1/2, z; (vii) x+1/2, y−1/2, z; (viii) x, −y, z; (ix) x+1, y, z+1; (x) x−1/2, y−1/2, z; (xi) x, y, z+1; (xii) x, −y, z+1; (xiii) x−1, y, z−1; (xiv) x+1/2, −y+1/2, z+1; (xv) x−1/2, y+1/2, z; (xvi) x+1/2, y−1/2, z+1.

Computational details.

To understand distributions of the paired electron densities around the isolated $[VO(O_2)_2CO_3]^{3-}$ complex anions, tight-binding linear muffin-tin orbital (TB-LMTO) calculations with the atomic sphere approximation (ASA) were carried out to evaluate electron localization function (ELF) using the Stuttgart TB-LMTO47 program. The local density approximation (LDA) was used for exchange and correlation, and all relativistic effects were taken into account using a scalar relativistic approximation except spin−orbit coupling. The valence electrons of the component elements were treated as O $2s^22p^4$, C $2s^22p^2$, V $3p^63d^34s^2$, and Cs $5s^25p^66s^2$. All subsequent calculations were performed on this optimized geometry. The plane-wave energy cutoff was set as 600 eV. The self-consistent convergence of the total energy was set as 2.0×10^{-6} eV/atom. The *k*-points sampling in the Brilliouin zone were set to be 3 × 3 × 4 according to the Monkhorst-Pack scheme.

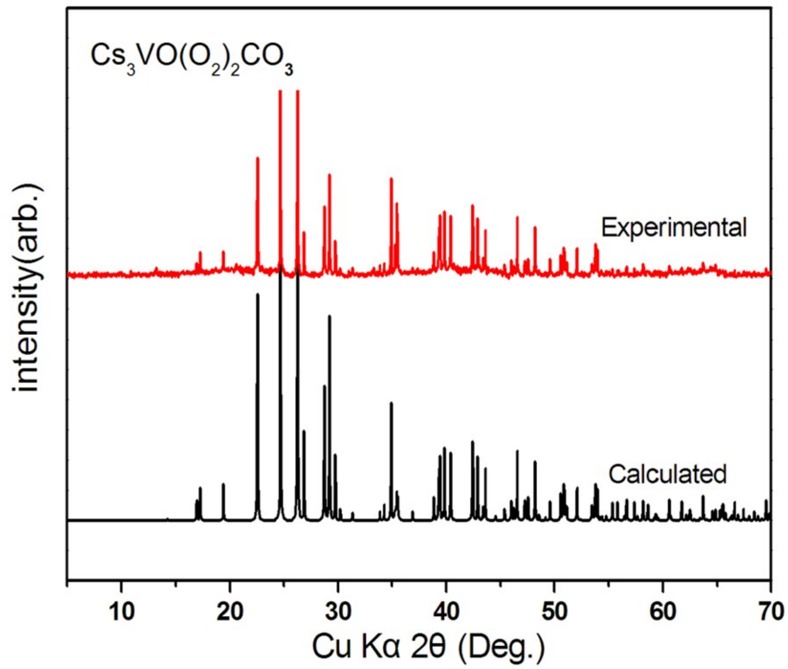

Fig. S2. Calculated and experimental powder X-ray diffraction (PXRD) patterns for $Cs_3VO(O_2)_2CO_3$

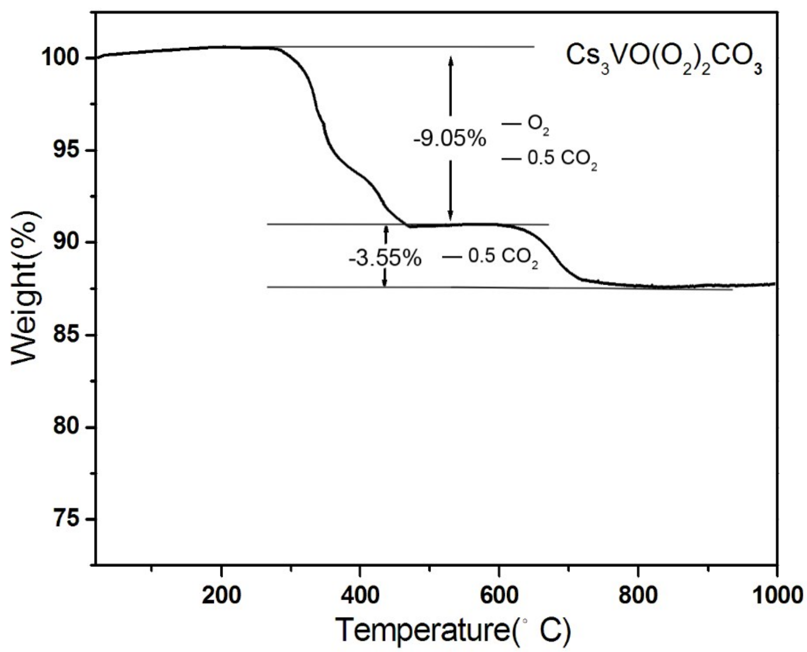

Fig. S3. Thermogravimetric analysis (TGA) diagram for $Cs_3VO(O_2)_2CO_3$

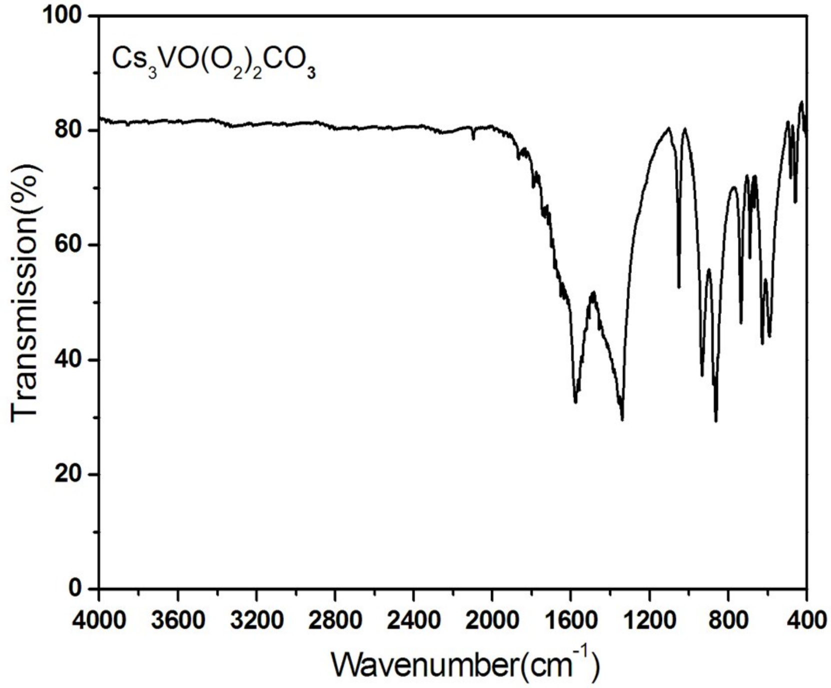

Fig. S4. IR spectrum for $Cs_3VO(O_2)_2CO_3$

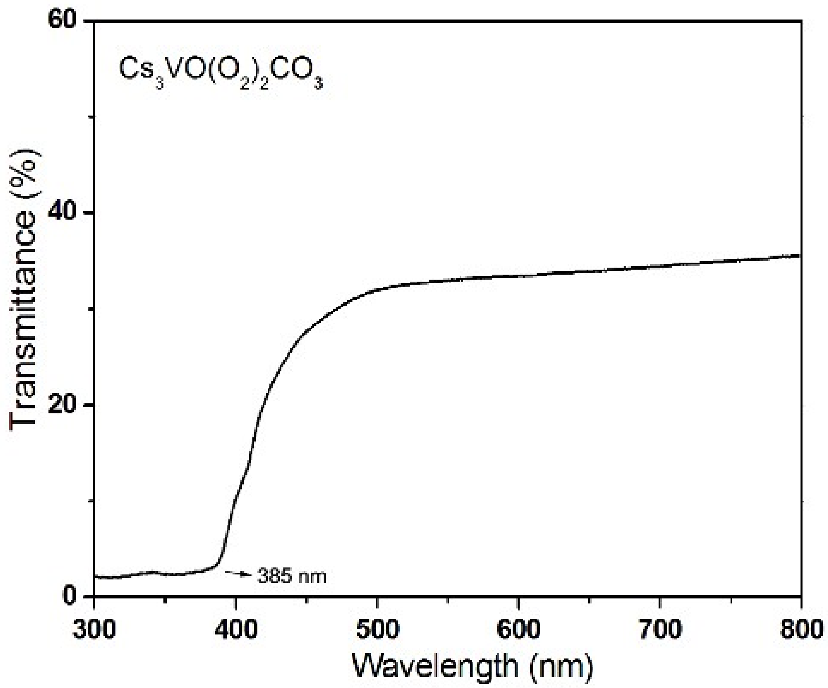

Fig. S5. Transmittance spectrum for $Cs_3VO(O_2)_2CO_3$

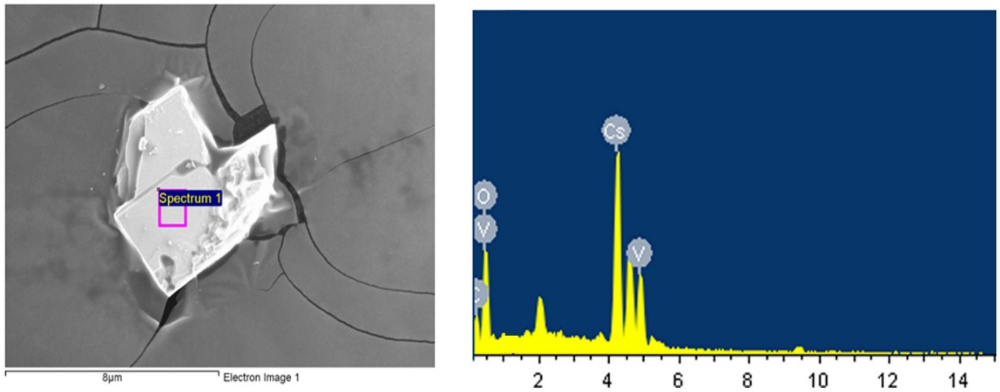

Fig. S6. Energy-dispersive analysis by X-ray (EDX) for $Cs_3VO(O_2)_2CO_3$

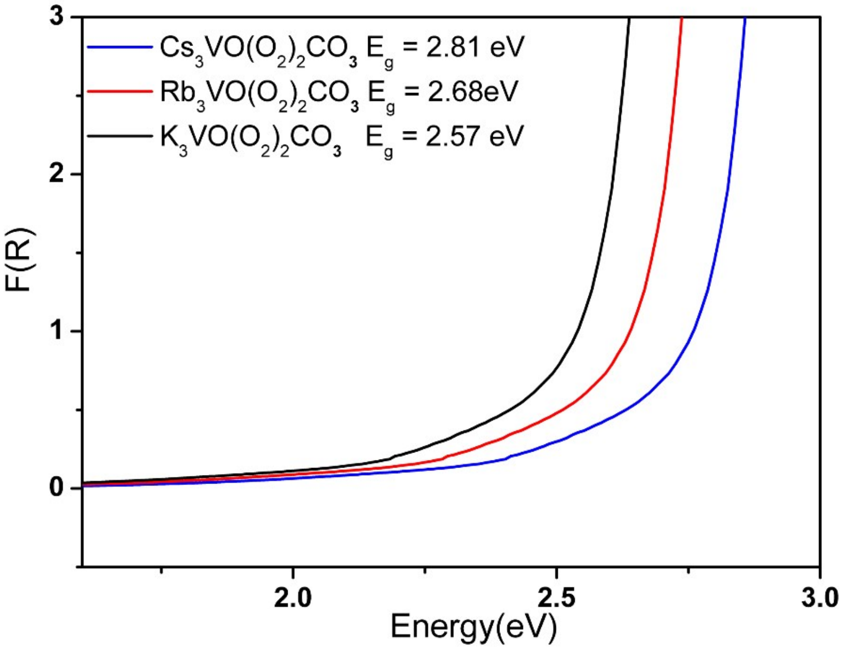

Fig. S7. The optical diffuse reflectance spectra for $A_3VO(O_2)_2CO_3$ (A = K, Rb, and Cs)

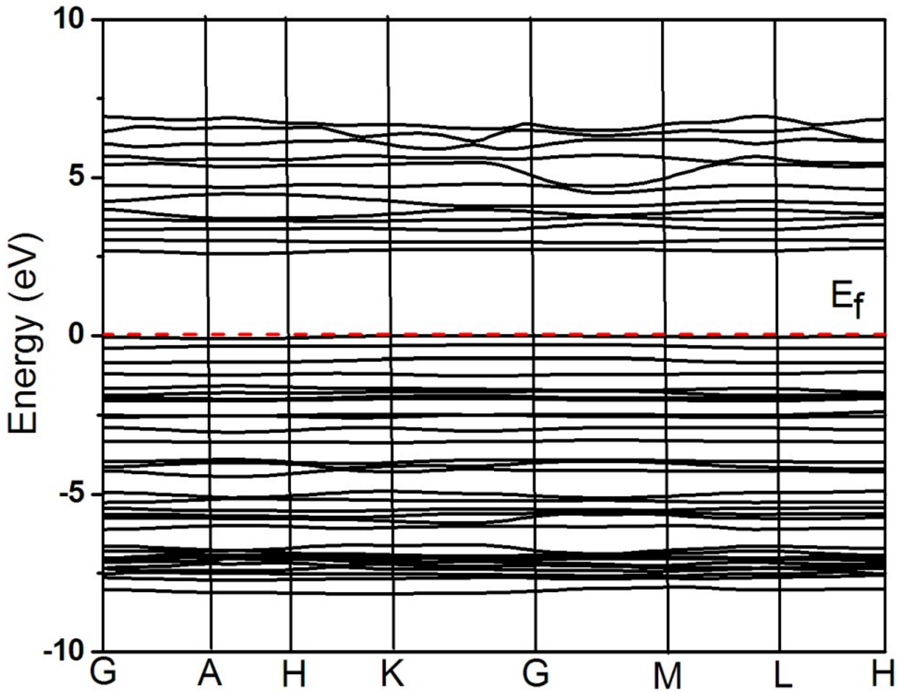

Fig. S8. Calculated band structure for $Cs_3VO(O_2)_2CO_3$ (the Fermi level is set at 0 eV)

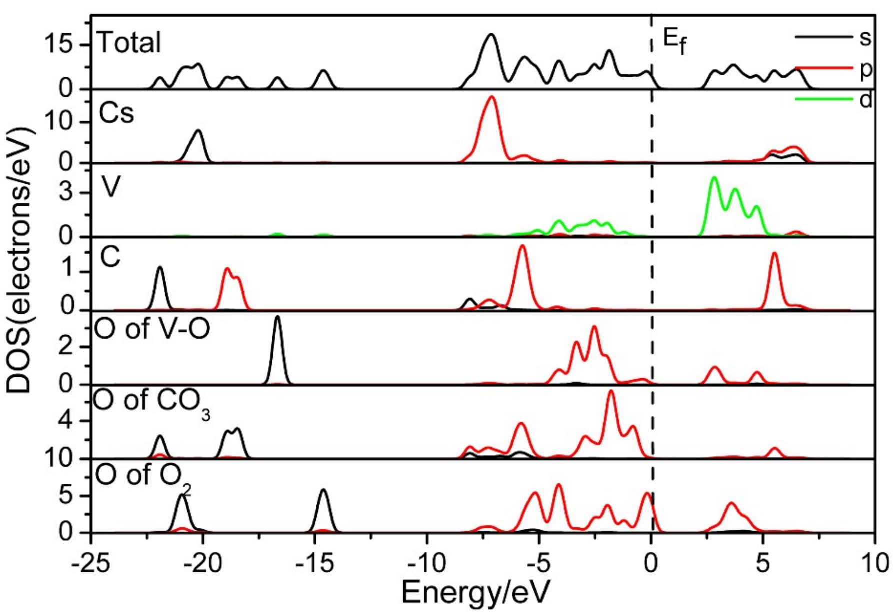

Fig. S9. Total and partial density of states for $Cs_3VO(O_2)_2CO_3$

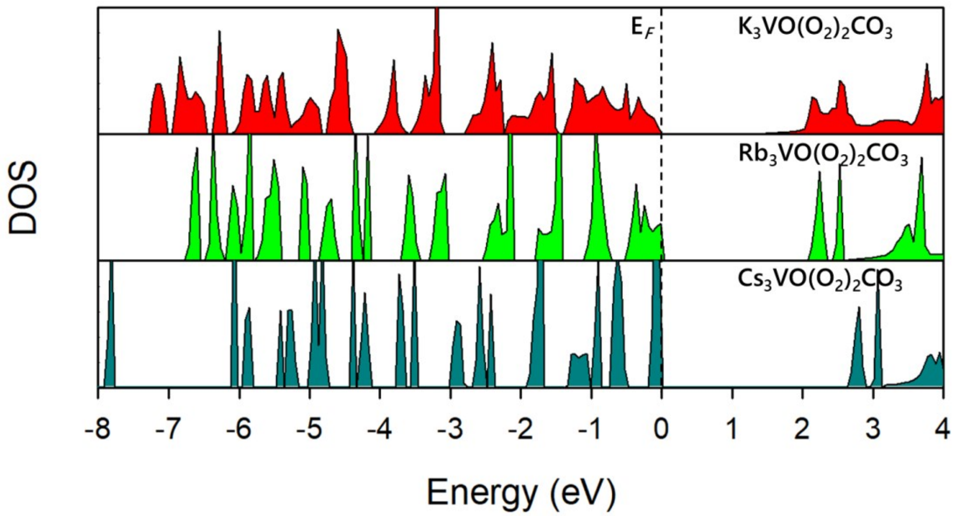

Fig. S10. Comparison of DOS curves for $A_3VO(O_2)_2CO_3$ (A = K, Rb, and Cs)

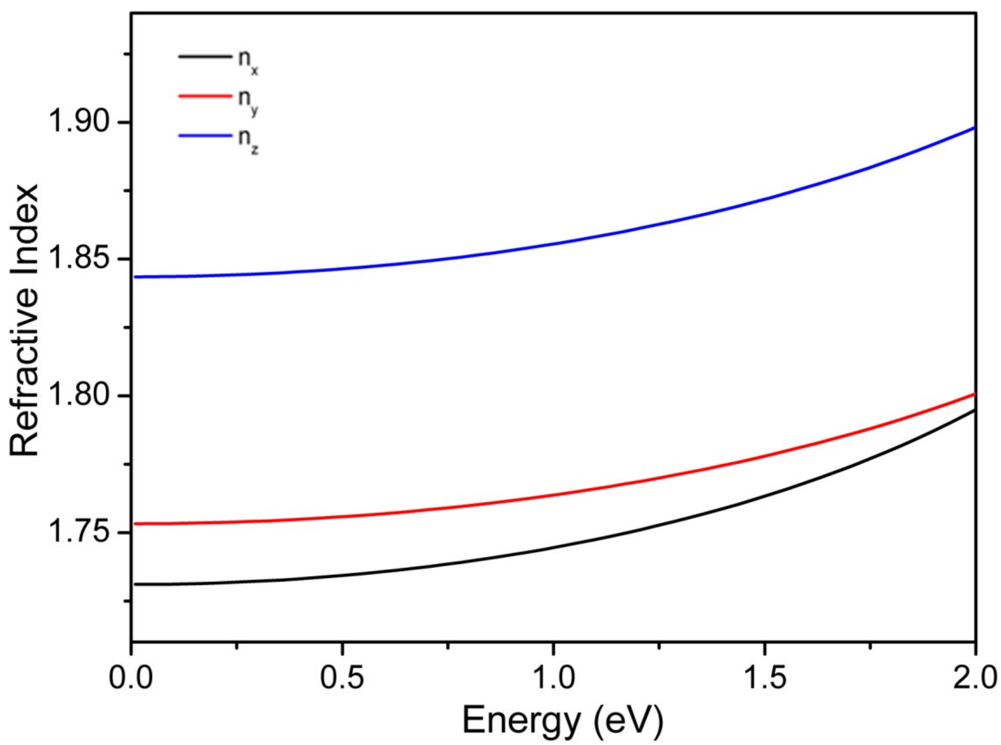

Fig. S11. Calculated refractive indexes for $Cs_3VO(O_2)_2CO_3$

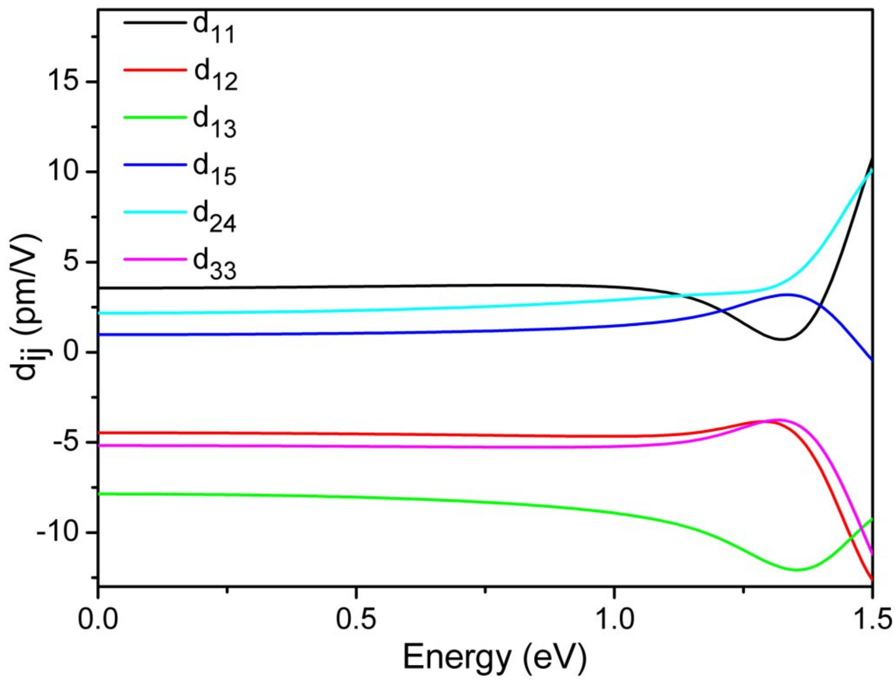

Fig. S12. Calculated frequency-dependent second-harmonic generation coefficients for $Cs_3VO(O_2)_2CO_3$

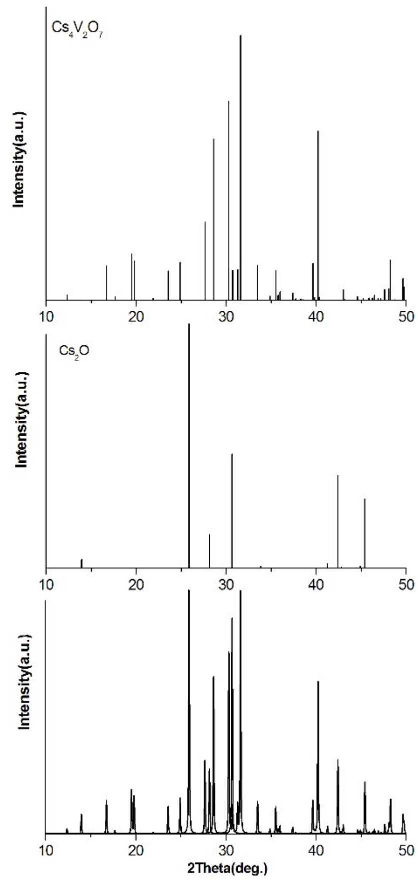

Fig. S13. Powder X-ray diffraction patterns for the thermally decomposed products of $Cs_3VO(O_2)_2CO_3$

References

S1. Sheldrick, G. M. *Acta Crystallog. Sect. A: Found. Crystallogr.* **2008**, *64*, 112.

S2. Spek, A. *J. Appl. Crystallogr.* **2003**, *36*, 7.

S3. Kubelka, P. *Z.Tech. Phys.* **1931**, *12*, 593.

S4. Tauc, J. *Mater. Res. Bull.* **1970**, *5*, 721.

S5. Ok, K. M.; Chi, E. O.; Halasyamani, P. S. *Chem. Soc. Rev.* **2006**, *35*, 710.